

Gas-phase SO₂ in absorption towards massive protostars^{*}

J. V. Keane¹, A. M. S. Boonman², A. G. G. M. Tielens^{1,3}, and E. F. van Dishoeck²

¹ Kapteyn Institute, PO Box 800, 9700 AV Groningen, The Netherlands

² Leiden Observatory, PO Box 9513, 2300 RA Leiden, The Netherlands

³ SRON, PO Box 800, 9700 AV Groningen, The Netherlands

Received 18 June 2001 / Accepted 11 July 2001

Abstract. We present the first detection of the ν_3 ro-vibrational band of gas-phase SO₂ in absorption in the mid-infrared spectral region around 7.3 μm of a sample of deeply embedded massive protostars. Comparison with model spectra shows that the derived excitation temperatures correlate with previous C₂H₂ and HCN studies, indicating that the same warm gas component is probed. The SO₂ column densities are similar along all lines of sight suggesting that the SO₂ formation has saturated, but not destroyed, and the absolute abundances of SO₂ are high ($\sim 10^{-7}$). Both the high temperature and the high abundance of the detected SO₂ are not easily explained by standard hot core chemistry models. Likewise, indicators of shock induced chemistry are lacking.

Key words. star-formation: gas-phase molecules – ISM: abundances – ISM: molecules

1. Introduction

Observations with the Infrared Space Observatory (*ISO*) have dramatically increased our knowledge of the active chemistry occurring within star-forming regions. Extensive studies have revealed a vast richness of solid-state molecules embedded in icy grain mantles (Ehrenfreund & Schutte 2000) which highlight the crucial role of grain surface chemistry in molecule formation. Paralleling this, the infrared and submillimeter (Boonman et al. 2000; Lahuis & van Dishoeck 2000; van der Tak et al. 2000a) observations of gas-phase molecules directly probe the chemical and physical conditions of the star-formation process. By combining the solid-state and gas-phase observations, a detailed picture of the evolving chemistry emerges which can serve as a stringent test of proposed chemical models of star-forming regions.

Sulphur-bearing species are particularly interesting to study as they were originally proposed as tracers of shocks since the increased availability of OH radicals will lead to enhanced abundances of specific molecular species (Hartquist et al. 1980). The chemistry of sulphur-bearing molecules in warm gas is essentially governed by neutral-neutral reactions involving H₂S formed on grain surfaces and subsequently evaporated into the gas-phase

(cf. Charnley 1997). The destruction of H₂S frees atomic sulphur, which can then readily react with OH and O₂ to produce SO. SO₂ is easily formed through the conversion of SO by OH. Above ~ 200 – 300 K, the OH radicals are driven into H₂O and the formation of SO₂ is halted. Except for the detection of the ν_3 band of gas-phase SO₂ in emission towards Orion (van Dishoeck et al. 1998), only purely rotational lines of SO₂ in the submillimeter have been detected toward massive star-forming regions. Abundances of $\sim 10^{-9}$ (Schreyer et al. 1997) are typically derived which are much lower than model predictions (Charnley 1997). SO₂ abundances up to 10^{-7} are only found in Orion-KL in the so-called plateau gas associated with the low-velocity outflow (e.g. Blake et al. 1987; Sutton et al. 1995). This gas is known to contain high abundances of OH (Melnick et al. 1987), and hence, the formation of SO₂ is intimately connected with the availability of reactive OH.

Here we present the first detection of infrared gas-phase SO₂ in absorption in the ν_3 ro-vibrational band towards a sample of embedded massive protostars.

2. Observations and reduction

High resolution AOT 6 ($\lambda/\Delta\lambda \geq 1600$) grating mode observations of the massive protostars presented in this article were made with the Short Wavelength Spectrometer (SWS) on-board *ISO*. The ν_3 ro-vibrational mode of SO₂ lies within Band 2C which suffers from instrumental fringing of varying severity. In order to extract unimpeded SO₂ ν_3 absorption profiles, the fringes were corrected for by

Send offprint requests to: J. V. Keane,
e-mail: jacquie@astro.rug.nl

^{*} Based on observations with *ISO*, an ESA project with instruments funded by ESA Member States (especially the PI countries: France, Germany, The Netherlands and the UK) and with the participation of ISAS and NASA.

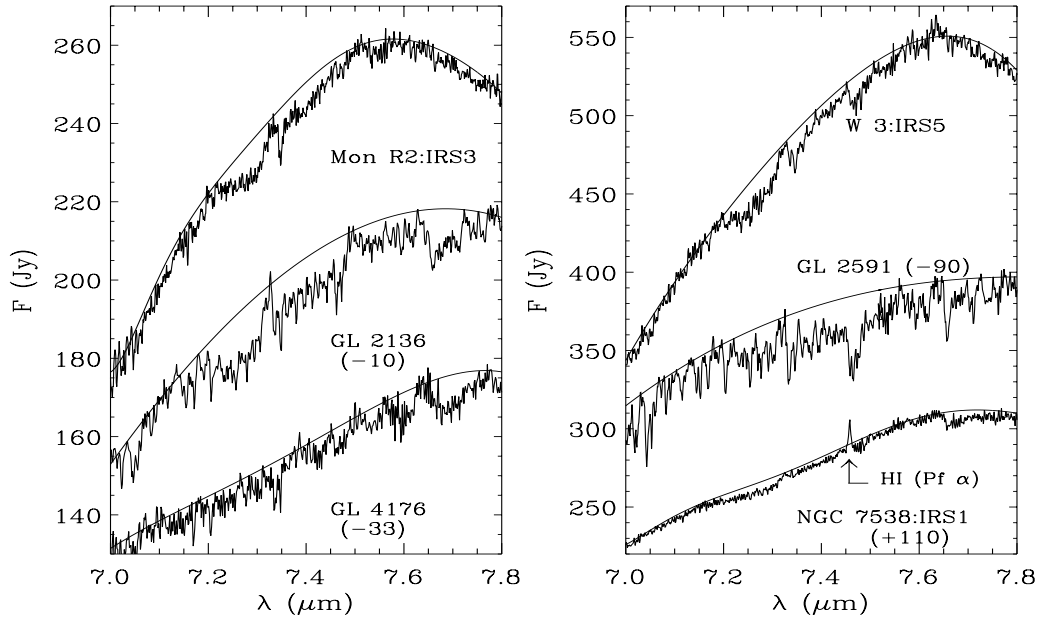


Fig. 1. ISO-SWS AOT 6 spectra towards six massive protostars. The thin solid lines indicate the locally defined 4th order polynomials adopted as the continua. Some of the sources were offset for clarity by a constant factor indicated in the brackets.

dividing the observed fluxes by cosine functions fitted to the data in wavenumber space (Lahuis & van Dishoeck 2000). The data were flat-fielded to the average level and then rebinned to the wavelength grid with a constant bin-size of $0.003 \mu\text{m}$ which corresponds to $\lambda/\Delta\lambda \sim 2500$. The fully reduced 7–8 μm spectra are shown in Fig. 1, where the noise level is approximately 4–5% for 3σ significance.

3. Absorption features

The 7–8 μm spectra (Fig. 1), towards all lines of sight, display a richness of broad and narrow absorption features attributable to solid-state and gas-phase molecular species. The region is dominated by the red wing of the 6.85 μm feature and the blue wing of the 10 μm silicate feature (Keane et al. 2001). The feature near 7.6 μm is well fitted by gas-phase and/or solid CH₄ (Boogert et al. 1997; Dartois et al. 1998). The spectra in Fig. 1 show evidence for weak features between 7.2 μm and 7.4 μm . The spectrum of Mon R2:IRS3 is particularly revealing in that it shows a narrow absorption feature at 7.342 μm flanked by broader red- and blue-shifted bands. This structure is reminiscent of the *P*, *Q*, and *R* branch structure of gaseous molecules. The other sources show similar structure albeit less pronounced due to the presence of gas-phase H₂O absorption lines (Boonman et al. 2000). A weak broad feature has been seen toward W 33A centered at 7.25 μm and has been attributed to solid HCOOH (Keane et al. in prep.). However, this feature is easily distinguished from the spectral structure observed here as it is shifted to the blue and cannot explain the observed *Q*- and *P*-branch structure. We attribute the spectral structure between 7.2 μm and 7.4 μm to gas-phase SO₂.

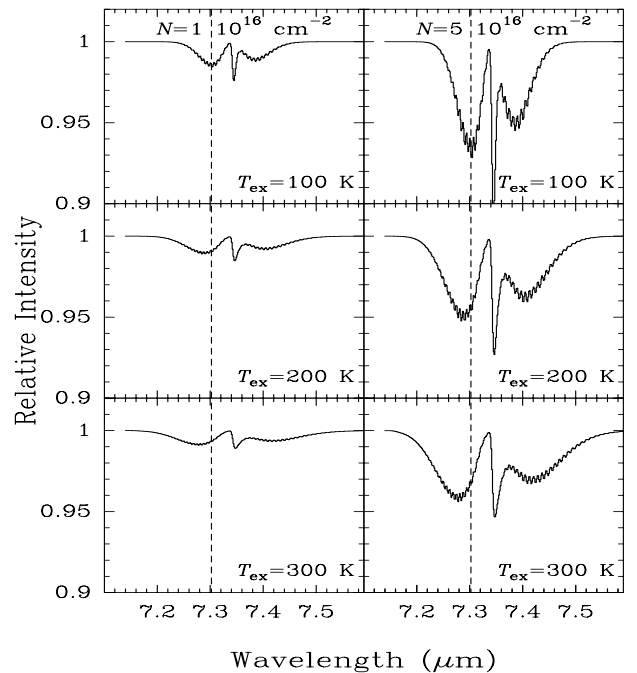


Fig. 2. Synthetic gas-phase SO₂ spectra calculated at various temperatures and column densities for a spectral resolution $R \sim 2000$. For all panels the Doppler parameter is 3 km s^{-1} . The dashed line shows the shift in the *R*-branch as a function of increasing excitation temperature.

4. Gas-phase SO₂

The modeling of the spectra has been performed using synthetic spectra from Helmich (1996) combined with the molecular line data from the HITRAN 2000 database (<http://www.hitran.com>). Following the same analysis as in Lahuis & van Dishoeck (2000) and Boonman et al. (2000) a homogeneous source has been assumed with a

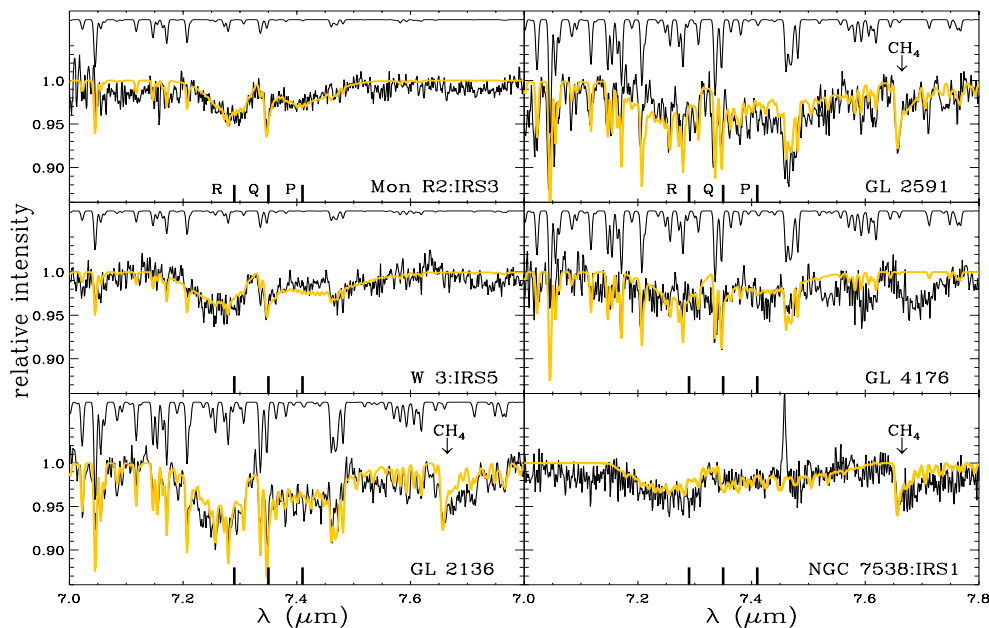


Fig. 3. The continuum divided spectra upon which the best fitting models (grey) are superimposed. Also shown are the H₂O model spectra (offset) used for the modeling except in the case of NGC 7538:IRS1. The position of the gas-phase CH₄ band is indicated for the sources where it was included in the modeling along with the SO₂ Q, R, and P branches (thick solid lines).

single temperature T_{ex} and column density N . Since the SO₂ models are not sensitive to the linewidth, a Doppler b parameter of 3 km s^{-1} is adopted here, corresponding to the mean value of the submillimeter SO₂ lines. Figure 2 illustrates the expected spectral structure of the ν_3 ro-vibrational band of gas-phase SO₂ for different column densities and excitation temperatures. A global comparison with the observations shows that the observed features imply typically a column of a few times 10^{16} cm^{-2} of warm ($\gtrsim 200 \text{ K}$) SO₂.

Using these models, we have made detailed fits to the observed absorption features. Half of the sources show the presence of strong gas-phase H₂O absorption in the ν_2 ro-vibrational band extending well into the $7.2\text{--}7.5 \mu\text{m}$ region. Therefore the H₂O model fits of Boonman et al. (2000) have been included in the modeling of gas-phase SO₂. In the sources GL 2591, NGC 7538:IRS1, and GL 2136 gas-phase CH₄ is also present and this has been included in the models, although it affects the SO₂ band only moderately ($\lesssim 2\%$). The best fitting models have been determined using the reduced χ^2_{ν} -method and are shown in Fig. 2. The corresponding excitation temperatures and column densities are listed in Table 1.

5. Discussion

Molecular abundances can serve as a direct means of probing the chemical history of star-formation. The derived SO₂ excitation temperatures range from $200\text{--}700 \text{ K}$ and are in good agreement with those inferred for HCN and C₂H₂ (Table 1), which are good tracers of warm gas (Lahuis & van Dishoeck 2000). The SO₂ column densities show little variation from source to source with typical

abundances of $4\text{--}8 \times 10^{-7}$ relative to the total H₂. The infrared SO₂ abundances are roughly consistent with the SO₂ abundances of $\sim 10^{-7}$ observed in the submillimeter towards the Plateau, the Compact Ridge, and the Hot Core in Orion (Sutton et al. 1995). The relative constancy of the Orion SO₂ abundances is striking given the physical differences that exist between the afore mentioned regions in Orion. On the other hand, the derived SO₂ abundances in hot cores are much higher than SO₂ abundances in dark clouds (Irvine et al. 1983). More recently, Hatchell et al. (1998) have found gas-phase SO₂ abundances of 5×10^{-10} to 2×10^{-8} in hot core regions, which are a factor of ≥ 10 less than what is derived here. Some of this difference may well reflect the beam dilution suffered by the submillimeter observations. Thus, given the Orion template, there are two possible origins for the high abundance of gaseous SO₂: hot core chemistry or shock induced chemistry.

In hot core chemistry, the SO₂ originates from oxidation of sulphur bearing species by OH (Charnley et al. 1997). This limits the SO₂ to gas with temperatures in the range ~ 100 to $\sim 200 \text{ K}$. The observed SO₂ temperature is well above this, though it is possible that this high temperature reflects radiative pumping by the dust. Moreover, HCN and C₂H₂ appear in gas with similar temperatures to that of the SO₂. This is difficult to reconcile since the formation of SO₂ becomes very inefficient for temperature above $\sim 230 \text{ K}$, whereas the route to HCN is greatly enhanced (Charnley 1997; Boonman et al. 2001; Rodgers & Charnley 2001). Thus, SO₂ cannot be abundant in gas which has become enriched in HCN through the removal of OH. The SO₂ and HCN abundances must therefore peak at different radii from the protostar in order for standard hot core models to be compatible. Alternatively, the SO₂

Table 1. SO₂ excitation temperatures and column densities in comparison with other gas-phase molecules.

Source	T_{ex} (K)					N (10^{16} cm ⁻²)						$\frac{N(\text{SO}_2)}{N(\text{H}_2)^c}$ 10^{-7}
	SO ₂	H ₂ O ^a	CO _{hot} ^b	HCN ^c	C ₂ H ₂ ^c	SO ₂	H ₂ O ^a	CO _{total} ^b	CO _{hot} ^b	HCN ^c	C ₂ H ₂ ^c	
Mon R2:IRS3	225 ⁺⁵⁰ ₋₇₀	300	310 ^d	—	—	4 ± 0.8	60	980 ^d	444 ^d	—	—	8.2
W 3:IRS5	450 ⁺¹⁰⁰ ₋₁₀₀	400	577	400	500	5 ± 0.8	40	2580	1260	0.5	0.3	3.8
GL 2136	350 ⁺⁵⁰ ₋₁₀₀	500	580	600	800	6 ± 0.8	150	2200	1500	3.5	1.5	5.5
GL 2591	750 ⁺⁷⁰ ₋₁₀₀	450	1010	600	900	6 ± 0.4	350	1280	558	4	2	6.3
GL 4176	350 ⁺¹⁷⁵ ₋₇₅	400	≥500 ^c	500	700	4 ± 1.0	150	1600 ^c	800 ^c	2	1	5.0
NGC 7538:IRS1	700 ⁺³⁰⁰ ₋₄₀₀	176 ^b	176	600	800	4 ± 1.0	<20	1740	840	1	0.8	4.7

^a Boonman et al. (2000) unless otherwise noted; ^b Mitchell et al. (1990) unless otherwise noted, using ¹³CO and assuming ¹²CO/¹³CO = 60; ^c Lahuis & van Dishoeck (2000); ^d Giannakopoulou et al. (1997).

may be formed on grains surfaces and then be released into the gas by evaporation. Grain surface chemistry models predict an abundance of $\sim 3 \times 10^{-3}$ relative to H₂O on the ice (Tielens & Hagen 1982; Tielens private communication), which is a factor $\gtrsim 10$ less than what is derived here. Another aspect is that the SO₂ column density does not vary between the sources, whereas H₂O shows large variation. The constancy of the SO₂ column density can be explained by the fact that the SO₂ is only abundant in a narrow zone between ~ 90 K (the ice evaporation temperature) and ~ 230 – 300 K (the OH \rightarrow H₂O transition), whose mass does not vary much in spite of the different total masses of the sources (Doty et al., in prep.).

The presence of SO and SO₂ has often been quoted as evidence for shocks (Hartquist et al. 1980). The degree to which the SO₂ abundance is enhanced depends on whether most of the sulphur is initially in atomic form ($\sim 10^{-7}$, Pineau des Forêts et al. 1993) or locked up in stable molecules ($\sim 10^{-8}$, Leen & Graff 1988). A good aspect of the shock induced chemistry hypothesis is that the SO₂ and HCN may be colocated in gas which contains freshly (i.e., $\lesssim 3.4 \times 10^4$ yr) released grain mantle molecules. However, the lack of increased SO₂ line widths at submillimeter wavelengths would seem to indicate the decay of shock activity within the region sampled by the submillimeter observations. In addition, the presence of fragile molecules sensitive to destruction by shocks (e.g. H₂CO; van der Tak et al. 2000b) makes shock-induced chemistry less likely as the source of SO₂ for these sources.

In general, the gaseous SO₂/H₂S ratio serves as a sensitive chemical clock for the star formation process and searches for these molecules at high spectral resolution are needed to help resolve the issue of the origin of the gas-phase SO₂.

Acknowledgements. The authors are grateful to F. Helmich for setting up the SO₂ synthetic spectra and to D. Kester for insightful discussions on fringe removal from ISO data. This work was supported by the Netherlands Organization for Scientific Research (NWO) through grant 614-041-003.

References

Allamandola, L. J., Sandford, S. A., Tielens, A. G. G. M., & Herbst, T. M. 1992, ApJ, 399, 134

- Blake, G. A., Sutton, E. C., Masson, C. R., & Phillips, T. G. 1987, ApJ, 315, 621
- Boogert, A. C. A., Schutte, W. A., Helmich, F. P., Tielens, A. G. G. M., & Wooden, D. H. 1997, A&A, 317, 929
- Boonman, A. M. S., van Dishoeck, E. F., Lahuis, F., Wright, C. M., & Doty, S. D. 2000, in ISO beyond the Peaks, ESA SP-456, 67 [astro-ph/0105249]
- Boonman, A. M. S., Stark, R., & van der Tak, F. F. S. 2001, ApJ, 553, L63
- Charnley, S. B. 1997, ApJ, 481, 396
- Dartois, E., D'Hendecourt, L., Boulanger, F., et al. 1998, A&A, 331, 651
- Ehrenfreund, P., & Schutte, W. A. 2000, in Astrochemistry: From molecular clouds to planetary systems, IAU Symp. 197, 135
- Giannakopoulou, J., Mitchell, G. F., Hasegawa, T. I., et al. 1997, ApJ, 487, 346
- Harquist, T. W., Oppenheimer, M., & Dalgarno, A. 1980, ApJ, 236, 182
- Hatchell, J., Thompson, M. A., Millar, T. J., & Macdonald, G. H. 1998, A&A, 338, 713
- Helmich, F. P. 1996, Ph.D. Thesis, Leiden
- Irvine, W. M., Good, J. C., & Schloerb, F. P. 1983, A&A, 127, L10
- Keane, J. V., Tielens, A. G. G. M., Boogert, A. C. A., et al. 2001, A&A, in press
- Lahuis, F., & van Dishoeck, E. F. 2000, A&A, 355, 699
- Leen, T. M., & Graff, M. M. 1988, ApJ, 325, 411
- Melnick, G. J., Genzel, R., & Lugten, J. B. 1987, ApJ, 321, 530
- Minh, Y. C., Ziurys, L. M., Irvine, W. M., & McGonagle, D. 1990, ApJ, 360, 136
- Mitchell, G. F., Maillard, J. P., Allen, M., Beer, R., & Belcourt, K. 1990, ApJ, 363, 554
- Pineau des Forêts, G., Roueff, E., Schilke, P., & Flower, D. R. 1993, MNRAS, 262, 915
- Rodgers, S. D., & Charnley, S. B. 2001, ApJ, 546, 324
- Schreyer, K., Helmich, F. P., van Dishoeck, E. F., & Henning, T. 1997, A&A, 326, 347
- Sutton, E. C., Peng, R., Danchi, W. C., et al. 1995, ApJS, 97, 455
- Tielens, A. G. G. M., & Hagen, W. 1982, A&A, 114, 245
- van der Tak, F. F. S., van Dishoeck, E. F., Evans, H. J. II, & Blake, G. A. 2000a, ApJ, 537, 283
- van der Tak, F. F. S., van Dishoeck, E. F., & Caselli, P. 2000b, A&A, 361, 327
- van Dishoeck, E. F., Wright, C. M., Cernicharo, J., et al. 1998, ApJ, 502, L173